

# NUCLEAR STRUCTURE CALCULATIONS WITH A VELOCITY DEPENDENT EFFECTIVE POTENTIAL FOR s-d AND p-f SHELL NUCLEI

BY M. Y. M. HASSAN, S. MOHARRAM, M. M. OSMAN AND H. M. ABDEL MONEM

Physics Department, Faculty of Science, Cairo University\*

(Received September 12, 1978; revised version received February 9, 1979)

Using a velocity dependent effective potential of s-wave interaction, Hartree-Fock calculations are performed for the doubly even  $N = Z$  nuclei from  $^{12}\text{C}$  to  $^{40}\text{Ca}$  and odd- $A$  nuclei in the 2p-1f shell. Values of the binding energy and the quadrupole moment are compared with previous calculations and with experimental data. Reasonable agreement is obtained for the calculated quantities as compared with previous results as well as with experimental data.

## 1. Introduction

Recently, a growing interest is directed to the use of Hartree-Fock (HF) calculations in studying the structure of light and heavy nuclei. In general, to do such calculations, two different types of interaction are used, namely realistic interaction and effective interaction. Some of these effective interactions are related to the realistic potentials and others are not directly related. Among those interactions which are related to the realistic potentials is the one derived by Dzhibuti and Mamasakhlisov [1]. They obtained their interaction by modifying the Serber force which describes well the nucleon-nucleon scattering at low energies. Dzhibuti and Sallam [2] used a modified form of this interaction to calculate the binding energies and the radii of a large group of nuclei from  $^4\text{He}$  to  $^{208}\text{Pb}$  and they obtained a good agreement with the experiment. Hassan et al. [3] have calculated the properties of nuclear matter using this effective potential and it was found that  $\text{BE}/A = -17.8 \text{ MeV}$  and  $k_F = 1.35 \text{ fm}^{-1}$ . Hassan and Ghazal [4] have performed single major shell HF calculations for s-d shell nuclei using this potential. The first part of the calculations of this paper deals with an extension of this work in which the assumption of inert

---

\* Address: Physics Department, Faculty of Science, Cairo University, Cairo, Egypt.

core is removed. Also, Hassan et al. [5] have studied even-even nuclei in the 2p-1f shell assuming  $^{40}\text{Ca}$  as an inert core. These calculations are extended to odd- $A$  nuclei in the second part of the present paper.

The general spirit of this work is to test the validity of the velocity dependent potential of s-wave interaction through the comparison of the calculated quantities for the nuclei considered with others as well as with the experimental data.

The method of calculation is given in Section 2, while Section 3 deals with the results and the discussion.

## 2. Method of calculation

### a) The effective two-body interaction

The effective two-body interaction is of the form [2]

$$V_{\text{eff}}(\vec{r}) = \frac{1}{2} \{ V_{\text{real}}(\vec{r}) \exp(-\vec{a} \cdot \vec{\nabla}) + \exp(\vec{a} \cdot \vec{\nabla}) V_{\text{real}}(\vec{r}) \}_{\vec{a} \rightarrow -\vec{a}} - \frac{\lambda(A)\hbar^2}{M} \{ \delta(\vec{r}) \nabla^2 + \nabla^2 \delta(\vec{r}) \}, \quad (1)$$

where the realistic potential  $V_{\text{real}}(\vec{r})$  is

$$V_{\text{real}}(\vec{r}) = [a_{\tau}(\vec{\tau}_1 \cdot \vec{\tau}_2) + a_{\sigma\tau}(\vec{\sigma}_1 \cdot \vec{\sigma}_2)(\vec{\tau}_1 \cdot \vec{\tau}_2)] \exp(-r^2/r_c^2), \quad (2)$$

$\sigma_i, \tau_i$  are the spin and isotopic spin operators. The parameters  $a_{\tau}$ ,  $a_{\sigma\tau}$  and  $r_c$  have been determined from the problem of free two-nucleon system and are found to be equal to:

$$a_{\tau} = 2.096 \text{ MeV}, \quad a_{\sigma\tau} = 7.767 \text{ MeV}, \quad r_c = 2.18 \text{ fm}. \quad (3)$$

### b) Calculations for even-even nuclei in the s-d shell

As a basis system we have the eigenfunctions of a harmonic oscillator with the oscillator  $\alpha = \sqrt{m\omega/\hbar}$  to fit the experimental root mean square radius of the nucleus. The basis system was truncated to include up to the third major shell.

A c. m. correction is introduced by subtracting the kinetic energy of the c. m. motion from the nuclear Hamiltonian and by minimizing the expectation value of this difference. The effect of the strength  $\eta$  of the spin-orbit force  $\vec{l} \cdot \vec{s}$  is also taken into consideration in our calculations.

As an initial guess in the variational calculations we used generalized Nilsson wave functions which were constructed to have the symmetries appropriate to our purpose.

The Coulomb effect is taken into consideration using the formula [2]:

$$E_c = 0.71Z^2/A^{1/3}.$$

The quadrupole moments are calculated according to the operator form:

$$\hat{Q}_{\lambda\mu} = \left[ \frac{4\pi}{2\lambda+1} \right]^{1/2} (\alpha r)^{\lambda} Y_{\lambda\mu}(\theta, \phi).$$

### c) Calculations for odd- $A$ nuclei in the p-f shell

The method of taking  $^{40}\text{Ca}$  as an inert core and performing the HF variation on the particles outside  $^{40}\text{Ca}$  which was applied previously by Hassan et al. [5] for even-even nuclei in the p-f shell is extended to odd-mass nuclei. The binding energies are corrected for Coulomb potential by adding a Coulomb energy of a uniform charge density [6] corresponding to the particles outside the core.

## 3. Results and discussion

### a) Even-even nuclei in the s-d shell

For these nuclei, the parameter  $\alpha$  is chosen to reproduce the experimental root mean square radius of each nucleus, while  $\lambda$  is adjusted to fit the experimental binding energy of  $^{40}\text{Ca}$ , this value of  $\lambda$  is taken as a constant for all nuclei and it is found to be  $-0.5 \text{ fm}^3$ . It is desirable to compare our results with some others that have appeared in the literature recently. The lowest energy HF solutions are given in Table I together with other calculated values. The values of the binding energy per particle as obtained in the present work (PW) show reasonable agreement with experiment. In the case of deformed nuclei, the deepest single-particle level is more bound than in the other calculations except the Lee and Cusson (LC) value, which agrees with our results. The last filled level for spherical nuclei is more bound than for deformed nuclei. This behaviour is observed in all types of calculation as can be seen from this table. The quality of agreement for the energy gap is about the same for all calculations. In Table II values of the charge quadrupole moment are given. The lowest energy solutions for the nuclei  $^{12}\text{C}$ ,  $^{20}\text{Ne}$ ,  $^{24}\text{Mg}$ ,  $^{28}\text{Si}$ ,  $^{32}\text{S}$  and  $^{36}\text{Ar}$  give the same experimental shape indicated by the charge quadrupole moments. However, their numerical values are much less than the experimental ones which result from using very small number of major shells, namely three major shells are considered. A remedy for the truncation of the space is to use different oscillator constants [10].

Volkov [15] has emphasized that a major factor causing the deformation of light nuclei is the decrease in the kinetic energy as the system is deformed. The effective kinetic energy gain is inversely proportional to the effective mass ratio  $m^*/m$ . It has been shown by Hassan et al. [3] that the effective mass ratio  $m^*/m$  is small for the interaction under consideration. This may explain why we obtained small values of the quadrupole moments.

The dependence of the binding energy and the energy gap, corresponding to the lowest energy solution for  $^{28}\text{Si}$  nucleus, on  $\eta$  is shown in figure 1. From this figure we notice that the binding energy increases with increasing  $\eta$  which agrees with previous calculations [8]. The energy gap is decreased by increasing  $\eta$ . The increase or the decrease of the gap depends on the nature of the lowest empty orbit which may change from one interaction to another.

As another test of the validity of the calculated radial functions obtained from this type of effective interaction, one may consider the density distribution of the  $^{40}\text{Ca}$  as an example. Comparison of the resulting density distribution with that obtained using different effective interactions: MDIK, B1, LINEG is shown in figure 2. The central density for B1 interaction is much higher than all the other densities. This can be attributed to the

TABLE I

Results of lowest energy HF solutions

	PW	MR	LC	FBB	MDIK	LINEG	ZR B <sub>I</sub>	Experiment [7]
<sup>12</sup> C (fm <sup>-1</sup> ) Deepest level last filled level <i>A</i> rms radius (fm) BE/ <i>A</i> (MeV)	0.620				-34.70	0.600	0.606	
	-65.60				8.40	10.14	17.40	
	-21.30				2.71	2.64	2.63	2.4 ± 0.03
	14.55				-6.88	-6.38	-5.15	-7.68
	2.37							
<sup>16</sup> O (fm <sup>-1</sup> ) Deepest level last filled level <i>A</i> rms radius (fm) BE/ <i>A</i> (MeV)	-8.88							
	0.568	0.568	0.602		-43.30	0.500	0.617	47
	-57.80	-71.40	-64.10					4.20
	-24.40	-24.80	-21.10		13.60	17.90	23.10	11.53
	10.78	19.50	20.60		2.73	2.65	2.65	2.67 ± 0.03
<sup>20</sup> Ne (fm <sup>-1</sup> ) Deepest level last filled level <i>A</i> rms radius (fm) BE/ <i>A</i> (MeV)	2.62	2.09	2.37		-7.95	-7.94	-5.81	-7.98
	-8.40	-8.14	-7.85					
	0.559	0.568	0.602	0.532	-46.00	0.545	0.569	
	-64.02	-56.40	-67.60	-46.10				
	-13.40	-12.70	-15.30	-7.90	6.20	7.20	15.10	10.11
<sup>24</sup> Mg (fm <sup>-1</sup> ) Deepest level last filled level <i>A</i> rms radius (fm) BE/ <i>A</i> (MeV)	7.22	6.20	9.70	7.03	3.07	2.96	2.96	2.91
	2.86	2.75	2.65	2.73	-7.50	-7.60	-5.51	-8.03
	-8.08	-6.13	-7.34	-2.00				
	0.547	0.568	0.602	0.478	-49.10	0.547	0.557	
	-68.10	-62.50	-70.60	-44.10				
<sup>24</sup> Mg (fm <sup>-1</sup> ) Deepest level last filled level <i>A</i> rms radius (fm) BE/ <i>A</i> (MeV)	-11.90	-14.40	-15.10	-4.56	2.80	5.00	12.10	9.21
	0.87	5.30	8.21	1.70	3.22	3.16	3.16	3.01 ± 0.03
	2.88	2.85	2.83	3.03	-7.53	-7.72	-5.49	-8.26
	-7.78	-6.78	-7.35	-1.70				

<sup>28</sup> Si (fm <sup>-1</sup> )	0.548	0.568	0.602	0.478					
Deepest level	-74.40	-68.80	-75.40	-48.70				0.559	
last filled level	-19.80	-18.40	-18.60	-8.50					
$\Delta$	7.77	7.50	8.80	7.24				13.31	8.68
rms radius (fm)	3.04	2.93	2.94	3.10				3.31	3.08 ± 0.06
BE/A (MeV)	-7.90	-7.79	-7.58	-2.19				-5.64	-8.45
<sup>32</sup> S (fm <sup>-1</sup> )	0.531	0.568	0.602	0.457				0.554	
Deepest level	-76.20	-74.00	-78.00	-48.95					
last filled level	-20.00	-19.20	-16.20	-6.10					
$\Delta$	2.30	4.50	7.70	1.02				11.10	6.43
rms radius (fm)	3.19	2.98	3.05	3.24				3.34	3.23 ± 0.07
BE/A (MeV)	-7.93	-8.70	-7.71	-2.02				-5.71	-8.49
<sup>36</sup> Ar (fm <sup>-1</sup> )	0.496	0.503	0.571					0.555	
Deepest level	-71.50	-59.30	-82.60						
last filled level	-21.40	-16.70	-18.30						
$\Delta$	1.30	5.30	8.60					12.10	6.48
rms radius (fm)	3.36	3.41	3.09					3.37	
BE/A (MeV)	-7.56	-6.80	-8.03					-5.95	-8.52
<sup>40</sup> Ca (fm <sup>-1</sup> )	0.492	0.503	0.571					0.570	
Deepest level	-74.80	-110.30	-87.60						-50 ± 11
last filled level	-26.23	-29.70	-21.20						-15.80
$\Delta$		23.70	18.40					20.50	7.27
rms radius (fm)	3.46	2.64	3.13					3.39	3.50
BE/A (MeV)	-8.47	-12.94	-8.44					-6.24	-8.55

$\Delta$  denotes the energy gap, PW — present work, MR — Reference [8], LR — Reference [9], FBB — Reference [10], MDIK — Reference [11], LINEG — Reference [12], BI — Reference [12].

TABLE II

The HF-charge quadrupole moments

Charge quadrupole moments $Q_0^c(\text{fm}^2)$								
Calculations	$^{12}\text{C}$	$^{20}\text{Ne}$	$^{24}\text{Mg}$	$^{28}\text{Si}_{\text{pr}}$	$^{28}\text{Si}_{\text{ob}}$	$^{32}\text{S}_{\text{pr}}$	$^{32}\text{S}_{\text{Tr}}$	$^{36}\text{Ar}$
PW	-9.9	4.8	12.5	20.0	-31.6	15.2	8.5	-9.2
MDIK	-19.5	53.5	68.9	88.6	-71.5	53.5	-61.8	-46.5
LINEG	-20.4	49.8	68.6	90.9	-72.2			-52.0
B1	-21.2	60.9	66.5	94.5	-71.6			-56.2
EXP. <sup>m</sup>	$-12.7 \pm 0.5$	$54 \pm 3$		$-55 \pm 2$		53		$54 \pm 6$
EXP. <sup>n</sup>	-20.1	$58 \pm 3$	$69 \pm 3$					
EXP. <sup>p</sup>	—	—	$85 \pm 12$	$-63 \pm 18$		$70 \pm 21$		$-39 \pm 21$

The notations are the same as in Table I, besides: <sup>m</sup> Reference [13], <sup>n</sup> Reference [14], <sup>p</sup> Reference [15].

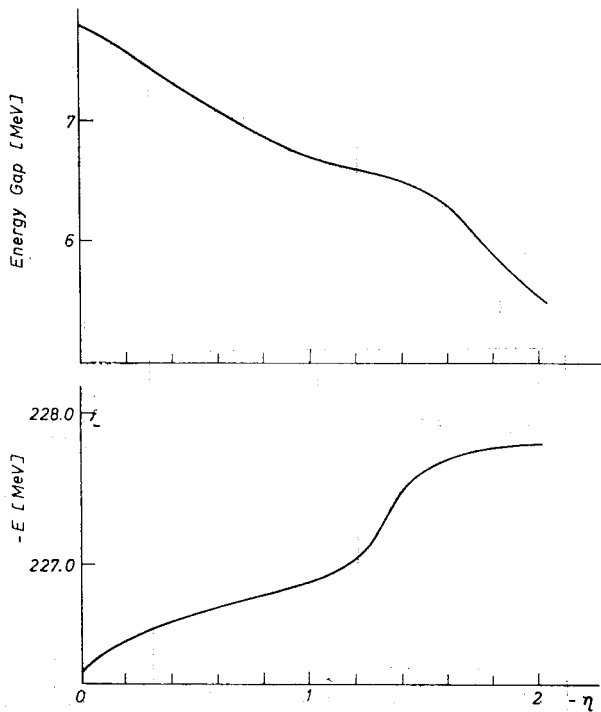


Fig. 1. The dependence of the lowest energy solution of  $^{28}\text{Si}$  on the spin-orbit strength  $\eta$  which is measured in the experimental units [11]

smallness of the compressibility corresponding to such interaction namely 193 MeV. The central density obtained in the present work is nearer to that of LINEG since the compressibility of LINEG force is 313 MeV and in our case it is found to be 261 MeV. The surface thickness is larger than in all other cases. The value of the compressibility has an effect on the surface thickness [16].

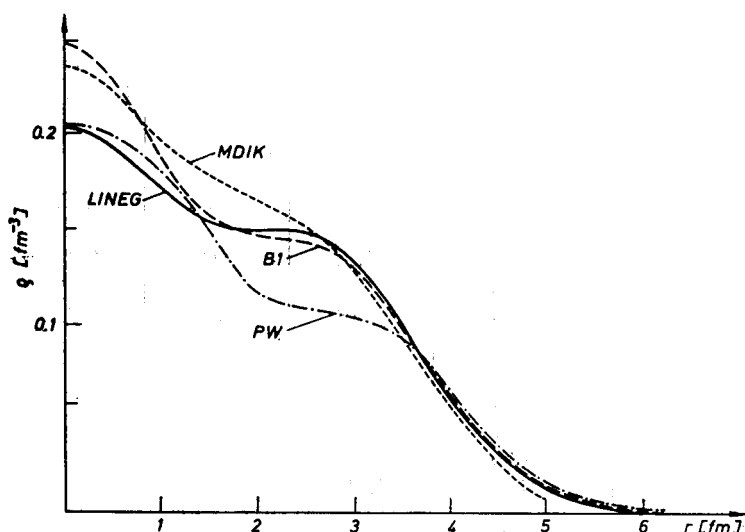


Fig. 2. The HF-density profiles for  $^{40}\text{Ca}$

#### b) Odd- $A$ nuclei in the 2p-1f shell

The results of even-odd nuclei are given in Tables IIIa, IVa. Inspection of these tables shows that:

##### (i) Titanium isotopes

The Ti isotopes have lowest energy solutions with axially prolate shape.  $^{49}\text{Ti}$  and  $^{51}\text{Ti}$  have two prolate solutions. The values of the HF-energies agree with SR results. The intrinsic quadrupole moments are small which means that the deformation is small. This result was obtained by Parikh [18] (JP1).

##### (ii) Chromium isotopes

The Cr isotopes have lowest energy solution with prolate shape. The HF energies agree with JP1 results and both are nearer to the experimental binding energies than SR calculations. The deformation of Cr isotopes are small as JP1 results in comparison with SR ones.

##### (iii) Iron isotopes

The lowest HF-solutions are with prolate shape for Fe isotopes. The values of the HF-energies are nearer to the experimental data than JP1 and SR results. The deformations are small with respect to SR results.

TABLE IIIa

Results for even-odd nuclei

Nucleus	Type	$-E_{HF}$	$E_c$	$-E_{HFB}$		BE
		PW		JP1	SR	EXP. [20]
<sup>47</sup> Ti	P	58.53	0.67	62.98	59.81	65.08
<sup>49</sup> Ti	P1	78.11	0.66	83.18	79.23	84.88
	P2	80.02				
<sup>51</sup> Ti	P1	100.58	0.66	101.78	97.24	102.18
	P2	97.82				
	O	99.10				
<sup>51</sup> Cr	P1	95.88	2.63	99.38	96.97	102.28
	P2	98.31				
<sup>53</sup> Cr	P	120.10	2.61	120.78	117.26	122.28
	O	117.82				
<sup>55</sup> Cr	P	139.08	2.59	140.28	135.39	138.18
<sup>55</sup> Fe	P1	136.49	5.82	137.98	131.91	138.98
	P2	138.80				
	O	136.24				
<sup>57</sup> Fe	P	162.92	5.77	159.88	153.20	157.68
<sup>65</sup> Zn	P	259.80	15.53	225.68		225.08
<sup>67</sup> Zn	P	286.71	15.42	248.88		243.18

JP1 — Reference [18], SR — Reference [19].

TABLE IIIb

Results for odd-even nuclei

Nucleus	Type	$-E_{HF}$	$E_c$	$-E_{HFB}$		BE
		PW		JP2	SR	EXP. [20]
<sup>49</sup> V	P1	74.95	1.50	81.2	77.44	83.4
	P2	77.78				
<sup>51</sup> V	P	98.86	1.48	101.2	97.89	103.7
<sup>53</sup> V	P	120.19	1.47	122.2	116.50	120.0
<sup>51</sup> Mn	P1	90.75	4.11	96.9	90.33	98.2
	P2	93.99				
<sup>53</sup> Mn	P1	116.09	4.08	120.6	114.02	120.8
	P2	119.15				
<sup>55</sup> Mn	P1	139.26	4.04	143.0	135.03	140.1
	P2	142.65				
<sup>55</sup> Co	P1	133.46	7.92	137.0		134.7
	P2	136.24				
<sup>57</sup> Co	P1	158.26	7.86	160.2	150.46	156.2
	P2	162.62				

JP2 — Reference [21].



TABLE IVa

The intrinsic quadrupole moments for even-odd nuclei

Nucleus	Type	( $Q_{20}$ ) HF	(Q <sub>20</sub> ) HFB	
		PW	JP1	SR
<sup>47</sup> Ti	P	0.46	0.29	0.96
<sup>49</sup> Ti	P1	0.46	0.26	0.99
	P2	0.39		
<sup>51</sup> Ti	P1	0.37	0.25	0.93
	P2	0.47		
	O	-0.27		
<sup>51</sup> Cr	P1	0.73	0.32	1.47
	P2	0.68		
<sup>53</sup> Cr	P	0.66	0.4	1.47
	O	-0.35		
<sup>55</sup> Cr	P	0.41	0.44	1.34
<sup>55</sup> Fe	P1	0.72	0.28	1.81
	P2	0.66		
	O	-0.30		
<sup>57</sup> Fe	P	0.57	0.42	1.60
<sup>65</sup> Zn	P	0.57	0.45	
<sup>67</sup> Zn	P	0.41	0.36	

TABLE IVb

The intrinsic quadrupole moments for odd-even nuclei

Nucleus	Type	( $Q_{20}$ ) HF	(Q <sub>20</sub> ) HFB	
		PW	JP2	SR
<sup>49</sup> V	P1	0.58	0.32	1.22
	P2	0.53		
<sup>51</sup> V	P	0.67	0.32	1.25
<sup>53</sup> V	P	0.50	0.31	1.18
<sup>51</sup> Mn	P1	0.72	0.40	1.63
	P2	0.67		
<sup>53</sup> Mn	P1	0.81	0.36	1.66
	P2	0.75		
<sup>55</sup> Mn	P1	0.64		1.6
	P2	0.58	0.36	
<sup>55</sup> Co	P1	0.89	0.42	
	P2	0.82		
<sup>57</sup> Co	P1	0.82	0.37	1.76
	P2	0.76		

## (iv) Zinc isotopes

Zn isotopes have prolate shape. The energies of the HF solutions are higher than the experimental binding energies. The deformations are small as in the case of Fe isotopes.

## Odd-even nuclei

The results for odd-even nuclei are shown in Tables IIIb, IVb; these tables show that for:

## (i) Vanadium isotopes

The lowest energy solution for V isotopes have prolate shape. The HF energies calculated by Parikh [21], (JP2) are in better agreement with experiment than ours. The values of the quadrupole moments are larger than JP2's values.

## (ii) Manganese isotopes

Mn isotopes have lowest energy solution with prolate shape. The quality of the agreement of HF energies with the experimental data is nearly the same as that obtained by JP2. The Mn isotopes are more deformed than V isotopes. The intrinsic quadrupole moments are larger than those calculated by JP2.

## (iii) Cobalt isotopes

The solutions of Co isotopes are prolate. The quality of the agreement of the HF energies compared to the experimental data is not much different from that obtained by JP2. The Co isotopes are more deformed than Mn isotopes.

In general, the addition of more neutrons to the even-even nuclei [5] considered in the p-f shell does not change the shape, except for Fe isotopes. The agreement of the calculated HF energies with the experimental data is not much different from other HFB calculations. The numerical values of the quadrupole moments are larger than HFB calculations of Parikh and are less than HFB calculations of Sandhu and Rustgi while the shape shows complete agreement.

In conclusion, reasonable results have been obtained compared to both experimental values and other calculations. However, this does not exclude trying to refine these calculations by enlarging the configuration space and by adding a p-state term or/and a density dependent term to the interaction.

## REFERENCES

- [1] R. I. Dzhibuti, V. I. Mamasakhlisov, *Soobshch. AN Gruz. SSR*, **54**, 57 (1969).
- [2] R. I. Dzhibuti, H. M. Sallam, *Yad. Fiz.*, **19**, 75 (1974).
- [3] M. Y. M. Hassan, A. Sh. M. Ghazal, K. M. H. Mahmoud, *Z. Phys.*, **A286**, 319 (1978).
- [4] M. Y. M. Hassan, A. Sh. M. Ghazal, *Acta Phys. Pol.*, **B10**, 77 (1979).
- [5] M. Y. M. Hassan, S. Moharram, H. M. Abdel Monem, to be published.
- [6] Gernot Eder, *Nuclear Forces*, the M.I.T. Press 1968.
- [7] R. Hofstadter, *Annu. Rev. Nucl. Sci.*, **7**, 231 (1959); C. S. Wu, *Annu. Rev. Nucl. Sci.*, **19**, 527 (1969); B. L. Cohen, *Phys. Rev.*, **130**, 227 (1963); G. Ripka, *Advances in Nuclear Physics*, **1**, 183 (1968), Plenum Press, New York; G. Ripka, *Lectures in Theoretical Physics*, ICTP Trieste 1967.
- [8] P. Mpanias, M. L. Rustgi, *Phys. Rev.*, **C12**, 2261 (1974).
- [9] H. C. Lee, R. T. Cusson, *Ann. Phys. (N.Y.)*, **72**, 353 (1972).
- [10] W. F. Ford, R. C. Bratly, J. Bar-Touv, *Phys. Rev.*, **C4**, 299 (1971).

- [11] K. R. Lassey, M. R. Manning, A. B. Volkov, *Can. J. Phys.* **51**, 2522 (1973).
- [12] J. Zofka, G. Ripka, *Nucl. Phys.* **A168**, 65 (1971).
- [13] J. Spech, G. R. Schweiner, H. Rabel, G. Schatz, R. Lohken, G. Hauser, *Nucl. Phys.* **A171**, 65 (1971).
- [14a] A. Nakada, Y. Torizuka, Y. Horikawa, *Phys. Rev. Lett.* **27**, 745 (1971).
- [14b] Y. Horikawa, Y. Torizawa, A. Nakada, S. Mitsunbu, Y. Kojima, M. Kimura, *Phys. Lett.* **B36**, 9 (1971).
- [15] K. Nakai, J. L. Qufbert, F. S. Stephens, R. M. Diamond, *Phys. Rev. Lett.* **24**, 903 (1970).
- [16] A. Volkov, *Nucl. Phys.* **74**, 33 (1965).
- [17] D. Vautherin, D. M. Brink, *Phys. Rev.* **C5**, 626 (1972).
- [18] J. K. Parikh, *Phys. Rev.* **C6**, 2177 (1972).
- [19] T. S. Sandhu, M. L. Rustgi, *Phys. Rev.* **C12**, 666 (1975).
- [20] R. A. Howard, *Nuclear Physics*, Wadsworth Publishing Company, INC. Blemot, California 1963.
- [21] J. K. Parikh, *Phys. Rev.* **C7**, 1864 (1973).